UNIVERSITÄT AUGSBURG
Universitätsbibliothek

OPEN ACCESS
OPUS AUGSBURG

Strain-controlled critical slowing down in the rheology of disordered networks

Jordan L. Shivers, Abhinav Sharma, Fred C. MacKintosh

Angaben zur Veröffentlichung / Publication details:

Shivers, Jordan L., Abhinav Sharma, and Fred C. MacKintosh. 2023. "Strain-controlled critical slowing down in the rheology of disordered networks." *Physical Review Letters* 131 (17): 178201. https://doi.org/10.1103/PhysRevLett.131.178201.

Nutzungsbedingungen / Terms of use:

licgercopyright

Dieses Dokument wird unter folgenden Bedingungen zur Verfügung gestellt: / This document is made available under these conditions:
Deutsches Urheberrecht
Weitere Informationen finden Sie unter: / For more information see:
https://www.uni-augsburg.de/de/organisation/bibliothek/publizieren-zitieren-archivieren/publiz/

Strain-Controlled Critical Slowing Down in the Rheology of Disordered Networks

Jordan L. Shivers,[1,2,*,†] Abhinav Sharma,[3,4] and Fred C. MacKintosh[1,2,5,6]
[1]Department of Chemical and Biomolecular Engineering, Rice University, Houston, Texas 77005, USA
[2]Center for Theoretical Biological Physics, Rice University, Houston, Texas 77005, USA
[3]Institute of Physics, University of Augsburg, 86159 Augsburg, Germany
[4]Leibniz-Institut für Polymerforschung Dresden, Institut Theorie der Polymere, 01069 Dresden, Germany
[5]Department of Chemistry, Rice University, Houston, Texas 77005, USA
[6]Department of Physics and Astronomy, Rice University, Houston, Texas 77005, USA

(Received 24 March 2022; revised 19 June 2023; accepted 25 September 2023; published 25 October 2023)

Networks and dense suspensions frequently reside near a boundary between soft (or fluidlike) and rigid (or solidlike) regimes. Transitions between these regimes can be driven by changes in structure, density, or applied stress or strain. In general, near the onset or loss of rigidity in these systems, dissipation-limiting heterogeneous nonaffine rearrangements dominate the macroscopic viscoelastic response, giving rise to diverging relaxation times and power-law rheology. Here, we describe a simple quantitative relationship between nonaffinity and the excess viscosity. We test this nonaffinity-viscosity relationship computationally and demonstrate its rheological consequences in simulations of strained filament networks and dense suspensions. We also predict critical signatures in the rheology of semiflexible and stiff biopolymer networks near the strain stiffening transition.

DOI: 10.1103/PhysRevLett.131.178201

Polymer gels, suspensions, emulsions, and foams are inherently composite in nature, with both elastic and fluidlike components [1,2]. In these systems, minor variations in parameters such as volume fraction [3–6], connectivity [7–12], and applied strain [13–15] can drive macroscopic transitions between fluidlike and solidlike behavior. These transitions are often heralded by familiar features of critical phenomena [16–18], including power-law scaling of relevant quantities with distance to a critical point [10,11,14,19,20] and diverging length and time-scales [21–27]. As a consequence of their disorder, these materials dissipate energy via heterogeneous or "nonaffine" deformation, such that microscopic and macroscopic deformation fields differ [9]. The associated microscopic nonaffine displacements can grow dramatically in magnitude near the onset or loss of rigidity and strongly influence macroscopic viscoelastic behavior [28–31]. However, these displacements are neglected in continuum models and are notoriously difficult to measure in experiments [32–34] except in special cases, such as confocal microscopy of colloidal suspensions [35–37].

Indirect evidence of nonaffinity can be seen experimentally, although specific rheological models are required to quantify this connection. Prior studies on dense suspensions [38–44], foams and emulsions [45,46], and immersed networks [28,29,47] have shown that a steady-state balance between externally applied power and the rate of dissipation by nonaffine rearrangement reveals phenomenological scaling relationships between the nonaffinity and loss modulus. This has even been used to identify critical exponents, e.g., for networks near isostaticity [29]. Yet, many systems, including biopolymer networks such as the cellular cytoskeleton and extracellular matrix, are subjected to large and often transient applied stresses and strains; in cells and tissues, this gives rise to highly strain-dependent and typically power-law rheology [48,49], the origins of which are not yet fully understood. Given the potential for large energy-dissipating nonaffine rearrangement near the onset of tension-dominated rigidity [14,50–53], one can assume that such rearrangements can lead to significant effects on network rheology in this regime. However, these effects remain poorly understood, especially in biopolymer or fiber systems with bending interactions, for which experimental measurement of nonaffinity has remained elusive.

Building on prior insights into the interplay between nonaffinity and energy dissipation, we identify a general relationship between the nonaffinity and measurable rheology of fluid-immersed networks. We find that the growth of nonaffine rearrangements near the strain stiffening transition drives a dramatic slowing down of stress relaxation in this regime. To explore the ensuing rheological consequences, we perform two- and three-dimensional simulations of prestrained disordered networks. We find that the longest relaxation time and nonaffinity both diverge as power laws with respect to distance to the stiffening transition. This leads to a set of scaling relations describing the relaxation modulus and nonaffinity near the critical strain, which we validate in simulations. We identify several experimentally testable

 © 2023 American Physical Society

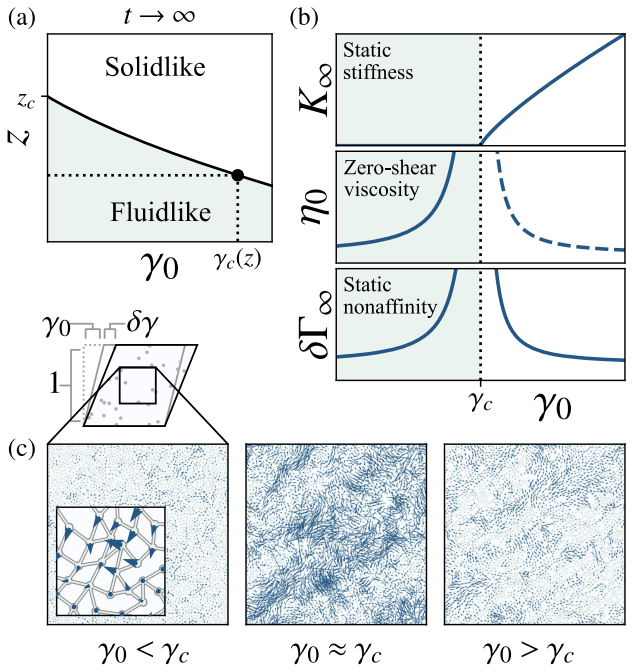

FIG. 1. (a) Immersed central-force spring networks with connectivity $z < z_c$ rigidify under shear strain γ_0 exceeding a z-dependent critical strain γ_c. (b) Rheological and kinematic features scale with the distance to the critical point, $|\gamma_0 - \gamma_c|$. At γ_c, the stiffness becomes nonzero, while the zero-shear viscosity and differential nonaffinity diverge. (c) Energy stored by an *affine* step strain $\delta\gamma$ is dissipated by microscopic nonaffine displacements $\boldsymbol{u}_i^{\mathrm{NA}}$, indicated here by arrows with uniformly scaled lengths.

predictions of this nonaffinity-dissipation relationship for a broad class of biopolymer and fiber systems.

We consider the overdamped dynamics of a d-dimensional system of N particles with positions $\boldsymbol{r}_i$ interacting via a potential energy $U = f(\boldsymbol{r}_1, \ldots, \boldsymbol{r}_N)$ [54]. These are immersed in a Newtonian fluid with velocity field $\boldsymbol{v}_f$, which imparts a drag force $\boldsymbol{f}_{d,i} = -\zeta[\dot{\boldsymbol{r}}_i - \boldsymbol{v}_f(\boldsymbol{r}_i)]$ that balances the interaction force $\boldsymbol{f}_{p,i} = -\partial U/\partial \boldsymbol{r}_i$, such that $\boldsymbol{f}_{d,i} + \boldsymbol{f}_{p,i} = \boldsymbol{0}$. This "free draining" description ignores long-range hydrodynamic interactions [55], which in our materials of interest can likely be neglected due to hydrodynamic screening. We apply macroscopic shear strain $\gamma(t)$ via Lees-Edwards periodic boundary conditions [56] and assume that the fluid deforms affinely, such that $\boldsymbol{v}_f(\boldsymbol{r}_i) = r_{i,z}\dot{\gamma}(t)\hat{\boldsymbol{x}}$; this is the widely used "affine solvent model" [5,21,29,39,40]. For a given strain rate $\dot{\gamma}$, the macroscopic shear stress is $\sigma = \eta_f\dot{\gamma} + (2V)^{-1}\sum_{ij} f_{ij,x} r_{ij,z}$, in which η_f is the fluid viscosity, V is the system's volume, the sum is taken over all pairs of interacting particles i and j, $\boldsymbol{f}_{ij}$ is the force on particle i due to particle j, $\boldsymbol{r}_{ij} = \boldsymbol{r}_j - \boldsymbol{r}_i$, and x and z denote the flow and gradient directions, respectively.

Nonaffinity quantifies the reorganization required for a system initially in mechanical equilibrium [satisfying force balance or, equivalently, minimizing $U(\boldsymbol{r}_i)$] to re-equilibrate after a small affine perturbation [57,58]. Consider an energy-minimized system at some prestrain γ_0, to which we apply an instantaneous affine strain step $\delta\gamma$ yielding transformed particle positions $\boldsymbol{r}_{i,0}$ with, in general, a net force on each particle. Evolving the equations of motion until the forces are once again balanced, we find that the particles take on new positions $\boldsymbol{r}_{i,\infty}$ defining static nonaffine displacements $\boldsymbol{u}_{i,\infty}^{\mathrm{NA}} = \boldsymbol{r}_{i,\infty} - \boldsymbol{r}_{i,0}$, as sketched in Fig. 1(c). These collectively define the static differential nonaffinity, $\delta\Gamma_\infty = (N\ell_0^2\delta\gamma^2)^{-1}\sum_i \|\boldsymbol{u}_{i,\infty}^{\mathrm{NA}}\|^2$. As noted earlier, in response to even small perturbations, amorphous materials near marginal stability tend to undergo large-scale rearrangement signaled by large $\delta\Gamma_\infty$.

We consider discrete elastic networks of central-force springs with stretching rigidity μ and angular springs with bending rigidity κ, prepared as described in Supplemental Material [59]. We focus on subisostatic networks, i.e., those with average connectivity z (number of bonds connected to each node) below Maxwell's d-dependent isostatic point $z_c = 2d$ [7]. For biopolymer networks, z is generally between 3 and 4 [72], far below z_c in $d = 3$. The linear elastic moduli of subisostatic networks, in the static ($t \to \infty$) limit, are proportional to κ. For $\kappa = 0$, they are thus *floppy* in the small strain limit [9] but can transition to a tension-stabilized rigid regime under finite applied strain. We select simple shear prestrain γ_0 as the rigidity control variable; in this case, static ($t \to \infty$) solidlike behavior develops when γ_0 reaches the z-dependent critical strain γ_c [10], as shown in Fig. 1(a). For $N, V \to \infty$, as γ_0 approaches γ_c, the system's zero-shear viscosity and nonaffinity diverge, as sketched in Fig. 1(b).

In Fig. 1(c), we plot static nonaffine displacement vectors for a representative network with $z = 3.5$ under varying prestrain. The nonaffine displacements are largest at the critical strain γ_c corresponding to the stiffening transition [50] [see Fig. 2(b)]. Although the corresponding maximum in the static nonaffinity $\delta\Gamma_\infty$ provides a clear signal of the critical point in simulations, its measurement in experiments, often by tracking embedded tracer particles [32–34], is challenging and limited in precision. Ideally, one could measure nonaffinity by relating it to more experimentally accessible quantities, such as the viscoelastic moduli. As noted earlier, such a relationship exists due to energy conservation: at steady state, the power injected into the system by the externally applied stress balances the power dissipated by the nonaffine rearrangement [28,29,38–47].

A similar power balance relates nonaffinity and viscoelasticity beyond the linear regime. Consider an energy-minimized configuration under prestrain $\gamma(t \le 0) = \gamma_0$ subjected to a superimposed oscillatory strain of amplitude $\delta\gamma$ and frequency ω, such that $\gamma(t) = \gamma_0 + \delta\gamma\sin(\omega t)$ for $t > 0$. After an initial transient regime, the stress steadily oscillates as $\sigma(t) = \sigma_0 + \delta\sigma\sin(\omega t + \theta)$, with amplitude $\delta\sigma$

and phase shift θ. Equivalently, $\sigma(t) = \sigma_0 + \delta\gamma[K'\sin(\omega t) + K''\cos(\omega t)]$, in which $K'(\gamma_0,\omega) = (\delta\sigma/\delta\gamma)\cos\theta$ and $K''(\gamma_0,\omega) = (\delta\sigma/\delta\gamma)\sin\theta$ are the frequency-dependent differential storage and loss moduli. For small $\delta\gamma$ [73], particles adopt elliptical trajectories $\boldsymbol{p}(t) = \boldsymbol{r}_i(t) - \boldsymbol{r}_{i,0}$ combining affine and nonaffine components $\boldsymbol{p}_i^{\mathrm{A}}(t) = \boldsymbol{u}_i^{\mathrm{A}}(\omega)\sin(\omega t + \theta^{\mathrm{A}})$ and $\boldsymbol{p}_i^{\mathrm{NA}}(t) = \boldsymbol{u}_i^{\mathrm{NA}}(\omega)\sin(\omega t + \theta^{\mathrm{NA}})$, with $\boldsymbol{p}(t) = \boldsymbol{p}^{\mathrm{A}}(t) + \boldsymbol{p}^{\mathrm{NA}}(t)$. The nonaffine displacement vectors collectively define the frequency-dependent nonaffinity, $\delta\Gamma(\omega) = (N\ell_0^2\delta\gamma^2)^{-1}\sum_i \|\boldsymbol{u}_i^{\mathrm{NA}}(\omega)\|^2$, in which ℓ_0 is a characteristic length scale, e.g., the typical spring length. The drag force on each particle is proportional to its velocity relative to the fluid, $\partial\boldsymbol{p}_i^{\mathrm{NA}}/\partial t = \omega\boldsymbol{u}_i^{\mathrm{NA}}(\omega)\times\cos(\omega t + \theta^{\mathrm{NA}})$. Averaged over each cycle, the external power input $P_{\mathrm{in}} = \frac{1}{2}V\omega d\gamma^2(K'' - \eta_f\omega)$ balances the total power output by nonaffine work, $P_{\mathrm{out}} = \frac{1}{2}N\omega^2\zeta\ell_0^2\delta\gamma^2\delta\Gamma(\omega)$ [59]. Thus, for any prestrain, we can express the differential dynamic viscosity $\eta'(\omega) = K''(\omega)/\omega$ in terms of the frequency-dependent nonaffinity as

$$\eta'(\omega) - \eta_f = \rho\zeta\ell_0^2\delta\Gamma(\omega) \tag{1}$$

in which $\rho = N/V$ is the particle number density. For $\omega \to 0$, this relates the zero-shear differential viscosity $\eta_0 = \lim_{\omega\to 0}\eta'(\omega)$ and the static nonaffinity $\delta\Gamma_\infty = \lim_{\omega\to 0}\delta\Gamma(\omega)$ as

$$\eta_0 - \eta_f = \rho\zeta\ell_0^2\delta\Gamma_\infty. \tag{2}$$

The latter indicates that, for a free-draining suspension with fluid viscosity η_f, the increase in zero-shear viscosity due to the presence of interacting particles, $\eta_0 - \eta_f$, is proportional to the fluid-independent static nonaffinity associated with the particle arrangement, $\delta\Gamma_\infty$. As this relationship is independent of U, it applies to a wide range of systems including, as we will later demonstrate, networks of bending-resistant filaments and soft sphere suspensions near jamming.

We now consider the effects of these relationships on the dynamic response of a strained network to an instantaneous strain step. To a relaxed system at prestrain γ_0, we apply an affine strain step $\delta\gamma$, such that $\gamma(t) = \gamma_0 + \delta\gamma$ for $t \geq 0$. The particles adopt nonaffine trajectories $\boldsymbol{u}_i^{\mathrm{NA}}(t) = \boldsymbol{r}_i(t) - \boldsymbol{r}_i(0)$ that collectively define the relaxation nonaffinity $\delta\Gamma(t) = (N\ell_0^2\delta\gamma^2)^{-1}\sum_i \|\boldsymbol{u}_i^{\mathrm{NA}}(t)\|^2$, for which $\delta\Gamma_\infty = \lim_{t\to\infty}\delta\Gamma(t)$. We measure the corresponding change in shear stress $\delta\sigma(t) = \sigma(t) - \sigma_0$ and compute the differential relaxation modulus $K(t) = \delta\sigma/\delta\gamma$ and differential zero-shear viscosity $\eta_0 - \eta_f = \int_0^\infty [K(t) - K_\infty]dt$, in which the static differential modulus is $K_\infty = \lim_{t\to\infty}K(t)$. Note that, for $\gamma_0 = 0$, K and $\delta\Gamma$ are the linear relaxation modulus $G(t) = \lim_{\gamma_0\to 0}K(t)$ and linear nonaffinity $\Gamma(t) = \lim_{\gamma_0\to 0}\delta\Gamma(t)$.

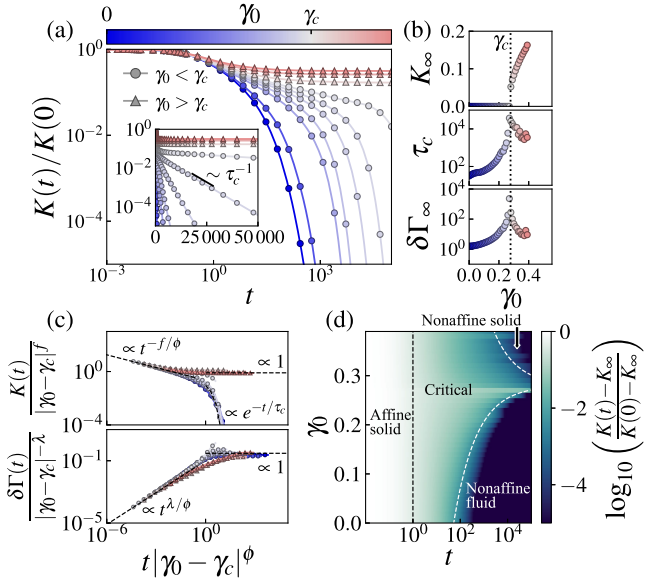

FIG. 2. When an immersed spring network at prestrain γ_0 is subjected to an instantaneous, infinitesimal strain increment $\delta\gamma$, (a) the relaxation modulus $K(t)$ decays to the static ($t \to \infty$) value K_∞ with a slowest relaxation time τ_c that (b) diverges at a critical prestrain $\gamma_0 = \gamma_c$ along with the static nonaffinity $\delta\Gamma_\infty$. (c) $K(t)$ and $\delta\Gamma(t)$ collapse according to the Widom-like scaling forms of Eqs. (3) and (4), with exponents $f = 0.7$, $\phi = 2.2$, and $\lambda = 1.5$. (d) Viscoelastic regimes on a (γ_0, t) phase diagram. Dashed white curves show $t \propto |\gamma_0 - \gamma_c|^{-\phi}$. Here, $N = 6400$, $z = 3.5$, $\tilde{\kappa} = 0$, and $\delta\gamma = 10^{-4}$.

Because the static nonaffinity $\delta\Gamma_\infty$ diverges at the critical strain, Eq. (2) implies that we should observe an equivalently diverging zero-shear viscosity and associated diverging slowest relaxation time. In Fig. 2(a), we plot stress relaxation curves for a single two-dimensional network with $z = 3.5$, with infinitesimal step strains applied over a range of prestrains γ_0 containing γ_c. The normalized relaxation modulus $K(t)/K(0) = \delta\sigma(t)/\delta\sigma(0)$ decays to its equilibrium value $K_\infty/K(0)$ with a γ_0-dependent slowest relaxation time τ_c (calculated as described in Supplemental Material [59]), which is plotted in Fig. 2(b) as a function of γ_0 along with the corresponding static nonaffinity $\delta\Gamma_\infty$, and static differential modulus $K_\infty = \delta\sigma_\infty/\delta\gamma$. Maxima in τ_c and $\delta\Gamma_\infty$ occur at the critical strain, where K_∞ becomes nonzero. We assign the exponent ϕ to the scaling of τ_c with $|\gamma_0 - \gamma_c|$ and, following Ref. [14], assign λ to $\delta\Gamma_\infty$ and f to K_∞.

The relaxation modulus exhibits power-law decay over a range of times extending from the microscopic relaxation time $\tau_0 = \zeta\ell_0/\mu = 1$ to a characteristic slow timescale governed by the distance from the critical strain, $\tau_c = |\gamma_0 - \gamma_c|^{-\phi}$. Within this regime, the relaxation modulus is a function of the ratio t/τ_c. Beyond τ_c, we expect the static critical behavior, i.e., $K_\infty \propto |\gamma_0 - \gamma_c|^f$ for $\gamma_0 \geq \gamma_c$. Thus, $K(t)$ should obey the scaling form

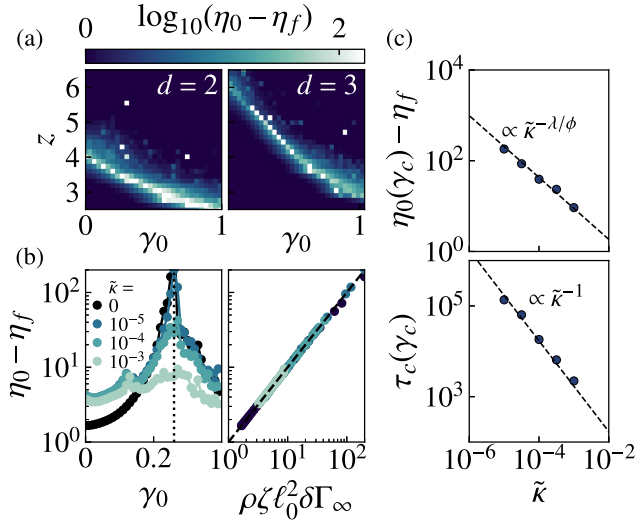

FIG. 3. In immersed networks, the zero-shear viscosity $\eta_0-\eta_f$ is maximized at the z-dependent critical strain γ_c, mirroring the nonaffinity. Here, $N(d=2)=10000$, $N(d=3)=8000$, and $\tilde{\kappa}=0$. (b) Finite bending rigidity $\tilde{\kappa}$ suppresses the divergence of $\eta_0-\eta_f$ at γ_c, yet Eq. (2) remains satisfied. Here, $N=1600$. (c) Peaks in the viscosity and slowest relaxation time decay with $\tilde{\kappa}$ as predicted by Eqs. (5) and (6).

$$K(t)=|\gamma_0-\gamma_c|^f\mathcal{F}_\pm(t|\gamma_0-\gamma_c|^\phi) \tag{3}$$

in which the branches of the scaling function $\mathcal{F}_\pm(x)$ correspond to regimes above and below the critical strain. When $x\gg 1$, $\mathcal{F}_+(x)\sim$ constant and $\mathcal{F}_-(x)\sim\exp(-x)$, implying $K(t)\sim|\gamma_0-\gamma_c|^f$ above γ_c and $K(t)\sim|\gamma_0-\gamma_c|^f\exp(-t|\gamma_0-\gamma_c|^\phi)$ below γ_c. When $x\ll 1$, $K(t)$ remains finite and thus must be independent of $|\gamma_0-\gamma_c|$, so $\mathcal{F}_\pm(x)\sim x^{-f/\phi}$. Therefore, for $\gamma_0=\gamma_c$, the relaxation modulus is predicted to decay as $K(t)\propto t^{-f/\phi}$.

Near γ_c, the differential nonaffinity is controlled by the same diverging timescale τ_c, yet should eventually display the static critical behavior $\delta\Gamma\propto|\gamma_0-\gamma_c|^{-\lambda}$. We thus expect

$$\delta\Gamma(t)=|\gamma_0-\gamma_c|^{-\lambda}\mathcal{G}_\pm(t|\gamma_0-\gamma_c|^\phi) \tag{4}$$

in which, for $x\gg 1$, $\mathcal{G}_+(x)\sim$ constant and $\mathcal{G}_-(x)\sim$ constant. Because $\delta\Gamma(t)$ remains finite when $x\ll 1$, $\mathcal{G}_\pm(x)\sim x^{\lambda/\phi}$. Thus, for $\gamma_0=\gamma_c$, the nonaffinity grows as $\delta\Gamma(t)\propto t^{\lambda/\phi}$. We observe excellent collapse of $K(t)$ and $\delta\Gamma(t)$ according to these scaling forms with exponents $f=0.7$, $\phi=2.2$, and $\lambda=1.5$, as shown in Fig. 2 [74].

We next test Eq. (2), which relates the independently measured static nonaffinity $\delta\Gamma_\infty$ and zero-shear viscosity η_0. In Fig. 3(a), we demonstrate that, like $\delta\Gamma_\infty$, η_0 is maximized at the finite-strain phase boundary between the statically floppy and rigid regimes. In Fig. 3(b), we plot $\eta_0-\eta_f$ for networks with varying dimensionless bending rigidity $\tilde{\kappa}$ and observe, in agreement with Eq. (2), a divergence in $\eta_0-\eta_f$ at the critical strain that is suppressed by increasing $\tilde{\kappa}$, which acts as a stabilizing field [14]. In Supplemental Material [59], we verify that the same nonaffinity-viscosity relationship applies in dense suspensions of frictionless soft spheres, in which η_0 diverges at a critical volume fraction ϕ_c.

The aforementioned power balance connects the static scaling exponents, f and λ, and the dynamic exponent, ϕ. At γ_c, the relaxation modulus decays as $K(t)\sim t^{-f/\phi}$ and the nonaffinity grows as $\delta\Gamma(t)\sim t^{\lambda/\phi}$, so the corresponding frequency dependence of the complex modulus and nonaffinity must be $K^*(\omega)\sim\omega^{f/\phi}$ and $\delta\Gamma(\omega)\sim\omega^{-\lambda/\phi}$. The former implies $\eta'(\omega)\sim\omega^{f/\phi-1}$; hence, Eq. (1) implies $\phi=f+\lambda$. Consequently, the static scaling of the stiffness and nonaffinity controls ϕ and, by extension, the exponents f/ϕ and λ/ϕ describing the system's stress relaxation and time-dependent rearrangement, as prior work has noted for networks near isostaticity [29]. Alternatively, we can rationalize this finding with a more qualitative argument: the relaxation time of large structural rearrangements scales with the "size" of these rearrangements, i.e., $\delta\Gamma_\infty\sim|\Delta\gamma|^{-\lambda}$, divided by the magnitude of their driving force, proportional to $K_\infty\sim|\Delta\gamma|^f$; hence, $\tau_c\sim|\Delta\gamma|^{-(\lambda+f)}$, with units set by the fluid viscosity. This relationship implies that the dynamic exponent ϕ is identical to the exponent describing the critical coupling to the bending rigidity, defined in Ref. [14]. Therefore, at γ_c, the excess zero-shear viscosity should scale with $\tilde{\kappa}$ just as $\delta\Gamma_\infty$ does [75],

$$\eta_0(\gamma_c)-\eta_f\propto\tilde{\kappa}^{-\lambda/\phi}, \tag{5}$$

and the slowest relaxation time should scale as

$$\tau_c(\gamma_c)\propto\tilde{\kappa}^{-1}, \tag{6}$$

independently of the critical exponents. These relationships are satisfied in simulations, as shown in Fig. 3(c).

Several of our predictions are experimentally testable. For example, the exponents f and ϕ (and thus λ) can be estimated via quasistatic strain-controlled rheology, as shown using reconstituted collagen networks in Ref. [14], after which the predicted scaling of $\eta'(\omega)$ for networks at γ_c, $\eta'(\omega)\propto\omega^{f/\phi-1}$, can be tested via small-amplitude oscillatory rheology at finite prestrain, i.e., $\gamma(t)=\gamma_0+\delta\gamma\sin(\omega t)$. In addition, η_0 and τ_c can be determined via step-strain stress relaxation tests, with $\gamma(t)=\gamma_0$ for $t<0$ and $\gamma(t)=\gamma_0+\delta\gamma$ for $t\geq 0$, allowing for tests of the predictions $\eta_0-\eta_f\propto|\gamma_0-\gamma_c|^{f-\phi}$ and $\tau_c\propto|\gamma_0-\gamma_c|^{-\phi}$. In the same manner, the predicted dependence of η_0 and τ_c on $\tilde{\kappa}$ can be tested using reconstituted collagen networks of varying concentration c, for which prior work has shown $\tilde{\kappa}\propto c$ [14,76]; hence, one would expect $\eta_0(\gamma_c)-\eta_f\propto c^{-\lambda/\phi}$ and $\tau_c\propto c^{-1}$.

In conclusion, we have demonstrated that a fundamental quantitative relationship between nonaffine fluctuations

and excess viscosity controls the rheology of immersed networks near the onset of rigidity. Consequently, the phase boundary for strain-induced stiffening in subisostatic networks is accompanied by a diverging excess viscosity. Applying prestrain to such networks thus produces a dramatic slowing of stress relaxation that is nonetheless quantitatively predictable from quasistatic nonaffine fluctuations. We provided experimentally testable predictions for the dynamics of networks near γ_c, with broad implications for the rheology of biological materials. To emphasize the generality of the nonaffinity-viscosity relationship, we showed that it fully captures the diverging zero-shear viscosity in suspensions of soft frictionless spheres near jamming in two and three dimensions [59].

There is widespread interest in the rational design of materials with tunable viscoelasticity [77–79]. This generally involves adjusting aspects of a material's preparation, such as polymer concentration or particle volume fraction. However, the connection between nonaffine fluctuations and excess viscosity implies that, in fiber networks, one can generate dramatic changes in stress relaxation dynamics by simply applying external strain, without changing the underlying network structure. This suggests other avenues for tuning the dynamics of stress relaxation; for example, embedded force-generating components can drive macroscopic stiffening transitions and thus precisely control the nonaffinity [80]. Examples include cytoskeletal molecular motors [81–83], contractile cells [84–86], and inclusions driven to shrink by varying temperature [87] or rearrange under applied magnetic fields [88].

Additional work will be needed to characterize the effects of finite system size on nonaffinity-induced critical slowing down near the onset of rigidity. For networks at the critical strain with correlation length exponent ν, we expect $\tau_c(\gamma_c) \propto L^{\phi/\nu}$ and $\eta_0(\gamma_c) - \eta_f \propto L^{\lambda/\nu}$ [59], suggesting additional ways to identify ν and test the previously proposed hyperscaling relation, $\nu = (f+2)/d$ [75]. Other areas to investigate include the effects of hydrodynamic interactions near the critical strain, as these both increase nonaffinity near isostaticity [89] and couple with nonaffinity to produce an additional intermediate-frequency viscoelastic regime at small strains [90], and the effects of finite temperature: the Green-Kubo relations tie the stationary stress correlations to the zero-shear viscosity [91,92] and thus to the athermal static nonaffinity. We note also that the association of diverging nonaffine fluctuations with the onset of rigidity, coupled with their microscopic role in slowing stress relaxation, may account for prior observations of slow dynamics in disordered materials such as fractal colloidal gels [93,94] and crowded, prestressed living cells [95–98]. Finally, it remains to be seen whether connections between nonaffinity and slowing down might provide insight into the glass transition [23,99–104].

This work was supported in part by the National Science Foundation Division of Materials Research (Grant No. DMR-2224030) and the National Science Foundation Center for Theoretical Biological Physics (Grant No. PHY-2019745). J. L. S. acknowledges additional support from the Lodieska Stockbridge Vaughn Fellowship.

*Corresponding author: jshivers@uchicago.edu
†Present address: James Franck Institute and Department of Chemistry, University of Chicago, Chicago, Illinois 60637, USA.

[1] R. G. Larson, *The Structure and Rheology of Complex Fluids* (Oxford University Press, New York, 1999).
[2] D. T. Chen, Q. Wen, P. A. Janmey, J. C. Crocker, and A. G. Yodh, Annu. Rev. Condens. Matter Phys. **1**, 301 (2010).
[3] M. Mooney, J. Colloid Sci. **6**, 162 (1951).
[4] R. A. Bagnold, Proc. R. Soc. A **225**, 49 (1954).
[5] D. J. Durian, Phys. Rev. Lett. **75**, 4780 (1995).
[6] J. Paredes, M. A. J. Michels, and D. Bonn, Phys. Rev. Lett. **111**, 015701 (2013).
[7] J. C. Maxwell, London, Edinburgh, Dublin Philos. Mag. J. Sci. **27**, 294 (1864).
[8] M. F. Thorpe, J. Non-Cryst. Solids **57**, 355 (1983).
[9] S. Alexander, Phys. Rep. **296**, 65 (1998).
[10] M. Wyart, H. Liang, A. Kabla, and L. Mahadevan, Phys. Rev. Lett. **101**, 215501 (2008).
[11] C. P. Broedersz, X. Mao, T. C. Lubensky, and F. C. MacKintosh, Nat. Phys. **7**, 983 (2011).
[12] A. Zaccone and E. Scossa-Romano, Phys. Rev. B **83**, 184205 (2011).
[13] Maurice A. Biot, *Mechanics of Incremental Deformations* (John Wiley & Sons, New York, 1965).
[14] A. Sharma, A. J. Licup, K. A. Jansen, R. Rens, M. Sheinman, G. H. Koenderink, and F. C. MacKintosh, Nat. Phys. **12**, 584 (2016).
[15] M. Merkel, K. Baumgarten, B. P. Tighe, and M. L. Manning, Proc. Natl. Acad. Sci. U.S.A. **116**, 6560 (2019).
[16] K. G. Wilson, Sci. Am. **241**, 158 (1979).
[17] M. E. Fisher, Phys. Phys. Fiz. **3**, 255 (1967).
[18] L. P. Kadanoff, W. Götze, D. Hamblen, R. Hecht, E. A. S. Lewis, V. V. Palciauskas, M. Rayl, J. Swift, D. Aspnes, and J. Kane, Rev. Mod. Phys. **39**, 395 (1967).
[19] C. S. O'Hern, L. E. Silbert, A. J. Liu, and S. R. Nagel, Phys. Rev. E **68**, 011306 (2003).
[20] J. A. Drocco, M. B. Hastings, C. J. O. Reichhardt, and C. Reichhardt, Phys. Rev. Lett. **95**, 088001 (2005).
[21] T. Hatano, Phys. Rev. E **79**, 050301(R) (2009).
[22] P. Olsson, Phys. Rev. E **91**, 062209 (2015).
[23] D. Bonn, M. M. Denn, L. Berthier, T. Divoux, and S. Manneville, Rev. Mod. Phys. **89**, 035005 (2017).
[24] H. A. Vinutha, K. Ramola, B. Chakraborty, and S. Sastry, Granular Matter **22**, 16 (2019).
[25] K. N. Nordstrom, E. Verneuil, P. E. Arratia, A. Basu, Z. Zhang, A. G. Yodh, J. P. Gollub, and D. J. Durian, Phys. Rev. Lett. **105**, 175701 (2010).
[26] A. Ikeda, T. Kawasaki, L. Berthier, K. Saitoh, and T. Hatano, Phys. Rev. Lett. **124**, 058001 (2020).

[27] K. Saitoh, T. Hatano, A. Ikeda, and B. P. Tighe, Phys. Rev. Lett. **124**, 118001 (2020).
[28] B. P. Tighe, Phys. Rev. Lett. **109**, 168303 (2012).
[29] M. G. Yucht, M. Sheinman, and C. P. Broedersz, Soft Matter **9**, 7000 (2013).
[30] R. Milkus and A. Zaccone, Phys. Rev. E **95**, 023001 (2017).
[31] V. V. Palyulin, C. Ness, R. Milkus, R. M. Elder, T. W. Sirk, and A. Zaccone, Soft Matter **14**, 8475 (2018).
[32] Q. Wen, A. Basu, J. P. Winer, A. Yodh, and P. A. Janmey, New J. Phys. **9**, 428 (2007).
[33] J. Liu, G. H. Koenderink, K. E. Kasza, F. C. MacKintosh, and D. A. Weitz, Phys. Rev. Lett. **98**, 198304 (2007).
[34] A. Basu, Q. Wen, X. Mao, T. C. Lubensky, P. A. Janmey, and A. G. Yodh, Macromolecules **44**, 1671 (2011).
[35] P. Schall, D. A. Weitz, and F. Spaepen, Science **318**, 1895 (2007).
[36] V. Chikkadi, G. Wegdam, D. Bonn, B. Nienhuis, and P. Schall, Phys. Rev. Lett. **107**, 198303 (2011).
[37] V. Chikkadi and P. Schall, Phys. Rev. E **85**, 031402 (2012).
[38] B. P. Tighe, E. Woldhuis, J. J. C. Remmers, W. van Saarloos, and M. van Hecke, Phys. Rev. Lett. **105**, 088303 (2010).
[39] B. Andreotti, J.-L. Barrat, and C. Heussinger, Phys. Rev. Lett. **109**, 105901 (2012).
[40] E. Lerner, G. Düring, and M. Wyart, Proc. Natl. Acad. Sci. U.S.A. **109**, 4798 (2012).
[41] E. Woldhuis, V. Chikkadi, M. S. v. Deen, P. Schall, and M. v. Hecke, Soft Matter **11**, 7024 (2015).
[42] E. DeGiuli, G. Düring, E. Lerner, and M. Wyart, Phys. Rev. E **91**, 062206 (2015).
[43] H. Ikeda, J. Chem. Phys. **153**, 126102 (2020).
[44] H. Ikeda and K. Hukushima, Phys. Rev. E **103**, 032902 (2021).
[45] G. Katgert, B. P. Tighe, and M. Van Hecke, Soft Matter **9**, 9739 (2013).
[46] J. Boschan, S. A. Vasudevan, P. E. Boukany, E. Somfai, and B. P. Tighe, Soft Matter **13**, 6870 (2017).
[47] G. Düring, E. Lerner, and M. Wyart, Phys. Rev. E **89**, 022305 (2014).
[48] X. Trepat, L. Deng, S. S. An, D. Navajas, D. J. Tschumperlin, W. T. Gerthoffer, J. P. Butler, and J. J. Fredberg, Nature (London) **447**, 592 (2007).
[49] Y. Mulla, F. C. MacKintosh, and G. H. Koenderink, Phys. Rev. Lett. **122**, 218102 (2019).
[50] P. R. Onck, T. Koeman, T. van Dillen, and E. van der Giessen, Phys. Rev. Lett. **95**, 178102 (2005).
[51] E. M. Huisman, C. Storm, and G. T. Barkema, Phys. Rev. E **78**, 051801 (2008).
[52] M. Sheinman, C. P. Broedersz, and F. C. MacKintosh, Phys. Rev. E **85**, 021801 (2012).
[53] J. L. Shivers, S. Arzash, and F. C. MacKintosh, Phys. Rev. Lett. **124**, 038002 (2020).
[54] In the context of disordered elastic networks, these particles constitute the network nodes, while U defines their interactions (e.g., stretching interactions between bonded nodes).
[55] V. Shankar, M. Pasquali, and D. C. Morse, J. Rheol. **46**, 1111 (2002).
[56] A. W. Lees and S. F. Edwards, J. Phys. C **5**, 1921 (1972).
[57] A. Tanguy, J. P. Wittmer, F. Leonforte, and J.-L. Barrat, Phys. Rev. B **66**, 174205 (2002).
[58] B. A. DiDonna and T. C. Lubensky, Phys. Rev. E **72**, 066619 (2005).
[59] See Supplemental Material at http://link.aps.org/supplemental/10.1103/PhysRevLett.131.178201 for additional theory and simulation details, expanded collapse plots, and data for soft sphere suspensions, which includes Refs. [60–71].
[60] S. Arbabi and M. Sahimi, Phys. Rev. B **38**, 7173 (1988).
[61] J. D. Ferry, *Viscoelastic Properties of Polymers*, 3rd ed. (Wiley, New York, 1980).
[62] A. Ikeda, L. Berthier, and P. Sollich, Soft Matter **9**, 7669 (2013).
[63] T. Kawasaki, D. Coslovich, A. Ikeda, and L. Berthier, Phys. Rev. E **91**, 012203 (2015).
[64] P. Olsson, Phys. Rev. Lett. **122**, 108003 (2019).
[65] Y. Nishikawa, A. Ikeda, and L. Berthier, J. Stat. Phys. **182**, 37 (2021).
[66] M. Wang and J. F. Brady, Phys. Rev. Lett. **115**, 158301 (2015).
[67] F. Boyer, E. Guazzelli, and O. Pouliquen, Phys. Rev. Lett. **107**, 188301 (2011).
[68] W. B. Russel, N. J. Wagner, and J. Mewis, J. Rheol. **57**, 1555 (2013).
[69] D. J. Koeze, D. Vågberg, B. B. Tjoa, and B. P. Tighe, Europhys. Lett. **113**, 54001 (2016).
[70] A. Singh, C. Ness, R. Seto, J. J. de Pablo, and H. M. Jaeger, Phys. Rev. Lett. **124**, 248005 (2020).
[71] A. Stukowski, Model. Simul. Mater. Sci. Eng. **18**, 015012 (2009).
[72] S. B. Lindström, D. A. Vader, A. Kulachenko, and D. A. Weitz, Phys. Rev. E **82**, 051905 (2010).
[73] S. Dagois-Bohy, E. Somfai, B. P. Tighe, and M. v. Hecke, Soft Matter **13**, 9036 (2017).
[74] We note that the exponents f, ϕ, and λ here, which describe the scaling of various quantities with respect to $|\gamma_0 - \gamma_c|$ for $z < z_c$, need not be the same as the corresponding exponents with respect to $|z - z_c|$ for $\gamma_0 = 0$ in, e.g., Refs. [11,29]. In general, it has been observed that the values of the critical exponents for the isostatic point and strain-controlled transition are different, i.e. $f_\gamma \neq f_z$ and $\phi_\gamma \neq \phi_z$.
[75] J. L. Shivers, S. Arzash, A. Sharma, and F. C. MacKintosh, Phys. Rev. Lett. **122**, 188003 (2019).
[76] K. A. Jansen, A. J. Licup, A. Sharma, R. Rens, F. C. MacKintosh, and G. H. Koenderink, Biophys. J. **114**, 2665 (2018).
[77] C. Raffaelli and W. G. Ellenbroek, Soft Matter **17**, 10254 (2021).
[78] N. Y. C. Lin, C. Ness, M. E. Cates, J. Sun, and I. Cohen, Proc. Natl. Acad. Sci. U.S.A. **113**, 10774 (2016).
[79] O. Chaudhuri, L. Gu, D. Klumpers, M. Darnell, S. A. Bencherif, J. C. Weaver, N. Huebsch, H.-p. Lee, E. Lippens, G. N. Duda *et al.*, Nat. Mater. **15**, 326 (2016).
[80] M. Sheinman, C. P. Broedersz, and F. C. MacKintosh, Phys. Rev. Lett. **109**, 238101 (2012).

[81] G. H. Koenderink, Z. Dogic, F. Nakamura, P. M. Bendix, F. C. MacKintosh, J. H. Hartwig, T. P. Stossel, and D. A. Weitz, Proc. Natl. Acad. Sci. U.S.A. **106**, 15192 (2009).
[82] C. P. Broedersz and F. C. MacKintosh, Soft Matter **7**, 3186 (2011).
[83] S. Wang and P. G. Wolynes, Proc. Natl. Acad. Sci. U.S.A. **109**, 6446 (2012).
[84] K. A. Jansen, R. G. Bacabac, I. K. Piechocka, and G. H. Koenderink, Biophys. J. **105**, 2240 (2013).
[85] P. Ronceray, C. P. Broedersz, and M. Lenz, Proc. Natl. Acad. Sci. U.S.A. **113**, 2827 (2016).
[86] Y. L. Han, P. Ronceray, G. Xu, A. Malandrino, R. D. Kamm, M. Lenz, C. P. Broedersz, and M. Guo, Proc. Natl. Acad. Sci. U.S.A. **115**, 4075 (2018).
[87] G. Chaudhary, A. Ghosh, N. A. Bharadwaj, J. G. Kang, P. V. Braun, K. S. Schweizer, and R. H. Ewoldt, Macromolecules **52**, 3029 (2019).
[88] G. Chaudhary, N. A. Bharadwaj, P. V. Braun, and R. H. Ewoldt, ACS Macro Lett. **9**, 1632 (2020).
[89] M. Dennison and H. Stark, Phys. Rev. E **93**, 022605 (2016).
[90] D. Head and C. Storm, Phys. Rev. Lett. **123**, 238005 (2019).
[91] D. Levesque, L. Verlet, and J. Kürkijarvi, Phys. Rev. A **7**, 1690 (1973).
[92] P. B. Visscher, P. Mitchell, and D. Heyes, J. Rheol. **38**, 465 (1994).
[93] T. H. Larsen and E. M. Furst, Phys. Rev. Lett. **100**, 146001 (2008).
[94] S. Aime, L. Cipelletti, and L. Ramos, J. Rheol. **62**, 1429 (2018).
[95] B. Fabry, G. N. Maksym, J. P. Butler, M. Glogauer, D. Navajas, and J. J. Fredberg, Phys. Rev. Lett. **87**, 148102 (2001).
[96] P. Bursac, G. Lenormand, B. Fabry, M. Oliver, D. A. Weitz, V. Viasnoff, J. P. Butler, and J. J. Fredberg, Nat. Mater. **4**, 557 (2005).
[97] X. Trepat, G. Lenormand, and J. J. Fredberg, Soft Matter **4**, 1750 (2008).
[98] R. H. Pritchard, Y. Y. Shery Huang, and E. M. Terentjev, Soft Matter **10**, 1864 (2014).
[99] J. D. Stevenson, J. Schmalian, and P. G. Wolynes, Nat. Phys. **2**, 268 (2006).
[100] F. Léonforte, A. Tanguy, J. P. Wittmer, and J.-L. Barrat, Phys. Rev. Lett. **97**, 055501 (2006).
[101] V. Lubchenko and P. G. Wolynes, Annu. Rev. Phys. Chem. **58**, 235 (2007).
[102] G. Brambilla, D. El Masri, M. Pierno, L. Berthier, L. Cipelletti, G. Petekidis, and A. B. Schofield, Phys. Rev. Lett. **102**, 085703 (2009).
[103] M. Ballauff, J. M. Brader, S. U. Egelhaaf, M. Fuchs, J. Horbach, N. Koumakis, M. Krüger, M. Laurati, K. J. Mutch, G. Petekidis *et al.*, Phys. Rev. Lett. **110**, 215701 (2013).
[104] A. Ikeda, L. Berthier, and P. Sollich, Phys. Rev. Lett. **109**, 018301 (2012).